

Deep-Time Marine Sedimentary Element Database

Jiankang Lai¹, Haijun Song^{1*}, Daoliang Chu¹, Jacopo Dal Corso¹, Erik A. Sperling², Yuyang Wu^{1*}, Xiaokang Liu¹, Lai Wei³, Mingtao Li⁴, Hanchen Song¹, Yong Du¹, Enhao Jia¹, Yan Feng¹, Huyue Song¹, Wenchao Yu¹, Qingzhong Liang⁵, Xinchuan Li⁵, Hong Yao⁵

¹State Key Laboratory of Biogeology and Environmental Geology, School of Earth Sciences, China University of Geosciences, Wuhan 430074, China

²Department of Earth and Planetary Sciences, Stanford University, Stanford, CA 94305, USA.

³School of Future Technology, China University of Geosciences, Wuhan 430074, China

⁴School of Resources and Environment, Linyi University, Linyi 276000, China

⁵School of Computer Science, China University of Geosciences, Wuhan 430074, China

Corresponding authors: Haijun Song (haijunsong@cug.edu.cn), Yuyang Wu (wuyuyang@cug.edu.cn)

Abstract. Geochemical data from ancient marine sediments are crucial ~~for~~ studying palaeoenvironments, palaeoclimates, and element~~al~~ cycles. With increased accessibility to geochemical data, many databases have emerged. However, there remains a need for a more comprehensive database that focuses on deep-time marine sediment records. Here, we introduce the “Deep-Time Marine Sedimentary Element Database” (DM-SED). The DM-SED has been built upon the “Sedimentary Geochemistry and Palaeoenvironments Project” (SGP) database with the new compilation of ~~34,938~~34,874 data entries from 433 studies, totalling ~~63,691~~63,627 entries. The DM-SED contains ~~2,412,085~~2,522,255 discrete marine sedimentary data points, including major and trace elements and some ~~stable~~ isotopes. It includes ~~9,271~~9,207 entries from the Precambrian and 54,420 entries from the Phanerozoic, thus providing significant references for reconstructing deep-time Earth system evolution. The data files described in this paper are available at <https://doi.org/10.5281/zenodo.13898366>~~https://doi.org/10.5281/zenodo.14771859~~ (Lai et al., 2024Lai

30 [et al., 2025](#)).

31

32 **1 Introduction**

33 Geochemical data from deep-time marine sediments are fundamental for reconstructing the evolution of
34 the Earth system. By analysing the ~~concentrations~~ concentrations of chemical elements in sediments and their isotopic
35 compositions, we can reconstruct the past cycling of elements in the Earth's surface systems and reveal
36 ~~the evolution of Earth's surface systems through time~~ ~~Earth's evolution through time~~ (Large et al., 2015;
37 Reinhard et al., 2017; Farrell et al., 2021; Planavsky et al., 2023). For instance, total organic carbon
38 (TOC), phosphorus (P), biogenic barium (Ba_{bio}), copper (Cu), zinc (Zn), nickel (Ni), etc., enable
39 reconstructing marine primary productivity and carbon cycle ~~perturbations~~ ~~changes~~, thereby revealing
40 ~~mechanisms driving past climate fluctuations~~ ~~past climate change mechanisms~~ (Scott et al., 2013;
41 Schoepfer et al., 2015; Shen et al., 2015; Schoepfer et al., 2016; Xiang et al., 2018; Jin et al., 2020;
42 Tribovillard, 2021; Wang et al., 2022; Zhang et al., 2022; Li et al., 2023; Sweere et al., 2023; Zhao et al.,
43 2023). Elements such as uranium (U), vanadium (V), and molybdenum (Mo) can reveal how marine
44 redox conditions changed during critical periods in animal evolution, including mass extinctions and
45 evolutionary radiations (Algeo and Liu, 2020; Schobben et al., 2020; Stockey et al., 2024). Oxygen
46 isotopes ($\delta^{18}O$) ~~from fossilized marine organisms~~ ~~in the remains of marine fossil animals~~ can reveal
47 oceanic palaeo-temperature changes (Veizer and Prokoph, 2015; Song et al., 2019; Grossman and
48 Joachimski, 2020; Scotese et al., 2021; Judd et al., 2022). However, many geochemical studies [have](#)
49 focused on high-resolution research of limited time intervals and/or regions, and there is little
50 comprehensive exploration across large-scale geological time and globally.

51 Fortunately, with more journals and institutions adopting strict data archiving rules and promoting
52 adherence to FAIR (Findability, Accessibility, Interoperability, and Reusability) principles (Wilkinson
53 et al., 2016; "FAIR Play in Geoscience Data," 2019), a large amount of geochemical data has become
54 accessible, and sample meta-data records are more detailed. Several geochemical databases of varying
55 scales and foci have emerged, such as the following:

- 56 ● EarthChem, which covers igneous, sedimentary, and metamorphic rocks and comprises numerous
57 joint databases (<https://www.earthchem.org/>, last accessed: 16 July 2024).

- 58 ● Petrological Database of the Ocean Floor (PetDB), which includes elemental chemical, isotopic, and
59 mineralogical data of global ocean floor igneous rocks, metamorphic rocks, minerals, and inclusions
60 (<https://www.earthchem.org/petdb>, last accessed: 16 July 2024).
- 61 ● Geochemistry of Rocks of the Oceans and Continents (GEOROC), a comprehensive compilation of
62 chemical, isotopic, and other data on igneous rock samples, including whole rock, glass, mineral,
63 and inclusion analyses and metadata (<http://georoc.mpch-mainz.gwdg.de>, last access: 16 July 2024).
- 64 ● Data Publisher for Earth & Environmental Science (PANGAEA), which is used for archiving,
65 publishing, and disseminating georeferenced data from earth, environmental, and biodiversity
66 sciences and includes a large number of sediment core data (<https://www.pangaea.de>, last accessed:
67 16 July 2024).
- 68 ● Stable Isotope Database for Earth System Research (StabisoDB) containing $\delta^{18}\text{O}$ and $\delta^{13}\text{C}$ data for
69 more than 67,000 macrofossil and microfossil samples, including benthic and planktonic
70 foraminifera, benthic and nektonic mollusks, brachiopods, fish teeth, and conodonts
71 (<https://cnidaria.nat.uni-erlangen.de/stabisodb/>, last accessed: 16 July 2024).
- 72 ● Sedimentary Geochemistry and Paleoenvironments Project (SGP), which collects multi-proxy
73 sedimentary geochemical data with an emphasis on Neoproterozoic-Palaeozoic shale data in its first
74 data release (<https://sgp-search.io/>, last accessed: 12 June 2024).
- 75 ● NOAA and MMS Marine Minerals Geochemical Database, which contains geochemical analyses
76 and auxiliary information on present-day marine deposits of primarily ferromanganese nodules and
77 crusts, as well as some data for heavy minerals and phosphorites
78 (<https://www.ncei.noaa.gov/access/metadata/landing->
79 [page/bin/iso?id=gov.noaa.ngdc.mgg.geology:G01323](https://www.ncei.noaa.gov/access/metadata/landing-), last accessed: 7 January 2025).
- 80 ● An International Study of the Marine Biogeochemical Cycles of Trace Elements and Isotopes
81 (GEOTRACES), which provides hydrographical and marine geochemical data acquired over the
82 past decade (<https://www.geotraces.org/>, last accessed: 7 January 2025).
- 83 Many other government initiatives also host databases:
- 84 ● The United States Geological Survey (USGS) National Geochemical Database, an archive of
85 geochemical information and related metadata from USGS research (<https://www.usgs.gov/energy->
86 [and-minerals/mineral-resources-program/science/national-geochemical-database](https://www.usgs.gov/energy-and-minerals/mineral-resources-program/science/national-geochemical-database), last accessed: 16
87 July 2024).

88 ● The British Geological Survey (BGS), which provides data and information on UK geology,
89 boreholes, geomagnetism, groundwater, rocks, etc. (<http://www.bgs.ac.uk/>, last accessed: 16 July
90 2024).

91 ● The Australian National Whole Rock Geochemistry Database (OZCHEM), including chemical
92 compositions of rock, soil, and sediment samples (<https://ecat.ga.gov.au/geonetwork/srv/>, last
93 accessed: 16 July 2024).

94 ~~NOAA and MMS Marine Minerals Geochemical Database, which contains geochemical analyses~~
95 ~~and auxiliary information on present day marine deposits of primarily ferromanganese nodules and~~
96 ~~crusts, as well as some data for heavy minerals and phosphorites~~
97 ~~(https://www.ncei.noaa.gov/access/metadata/landing_~~
98 ~~page/bin/iso?id=gov.noaa.ngde.mgg.geology:G01323, last accessed: 7 January 2025).~~

99 ● ~~An International Study of the Marine Biogeochemical Cycles of Trace Elements and Isotopes~~
100 ~~(GEOTRACES), which provides hydrographical and marine geochemical data acquired over the~~
101 ~~past decade (<https://www.geotraces.org/>, last accessed: 7 January 2025).~~

102 Although some of these databases (Table 1) include data on ancient marine sediments, they have
103 shortcomings such as limited spatial coverage, the lack of age data and coarse age resolution, the absence
104 of recent publications, and missing information from original publications~~data on ancient marine~~
105 ~~sediments, they are often limited to specific countries or regions and have certain shortcomings, such as~~
106 ~~the lack of age data, the absence of many recent publications, missing information from original~~
107 ~~individual publications, and relatively coarse age resolutions.~~ Thus, we ~~propose~~have established the
108 Deep-Time Marine Sedimentary Element Database (DM-SED), which focuses on the elemental content
109 changes in marine sediments across geological history. The current version of the DM-SED database
110 contains ~~63,694~~63,627 entries, enabling research on a series of scientific issues related to
111 palaeoenvironmental, palaeoclimatic, and elemental cycles in deep-time Earth history.

112 DM-SED version 0.0.1 is presented in table (.csv) format. Dynamic versions of the most recent
113 release can be found on Zenodo (<https://doi.org/10.5281/zenodo.14771859>, last accessed: 30 January
114 2025) (Lai et al., 2025), and a static copy of Version 0.0.1 is archived in the Geobiology database
115 (<http://202.114.198.132/dmgeo-geobiology-portal/>, last accessed: 25 September 2024). In the following
116 sections, we provide a brief overview of the database, information on the data sources and selection
117 criteria, and a review of the definitions and decisions behind the metadata fields associated with each

118 proxy measurement. We explore the spatial and temporal distribution trends of the compiled data and
 119 discuss future uses and limitations of the database.

133 **Table 1. Overview of different databases (Note: not all databases have a clear number of records).**

Database name	Content	Website information	Number of records	Data regions
EarthChem	Igneous, sedimentary, and metamorphic rocks; various joint databases	https://www.earthchem.org/ , last accessed: 16 July 2024	Over 2,596 digital content files in EarthChem Library	Global
PetDB	Elemental chemical, isotopic, and mineralogical data of global ocean floor rocks	https://www.earthchem.org/petdb , last accessed: 16 July 2024	Over 6,000,000 samples	Global
GEOROC	Chemical, isotopic, and other data on igneous rock samples	http://georoc.mpch-mainz.gwdg.de , last access: 16 July 2024	672,990 samples	Global
PANGAEA	Georeferenced data from earth, environmental, and biodiversity sciences	https://www.pangaea.de , last accessed: 16 July 2024	Extensive dataset	Global
StabisoDB	$\delta^{18}\text{O}$ and $\delta^{13}\text{C}$ data for macrofossil and microfossil samples	https://cnidaria.nat.uni-erlangen.de/stabisodb/ , last accessed: 16 July 2024	Over 67,000 samples	Global

SGP	Multi-proxy sedimentary geochemical data from the Palaeozoic and Neoproterozoic	https://sgp-search.io/ , last accessed: 12 June 2024	82,578 samples	Global
NOAA and MMS Marine Minerals Geochemical Database	Geochemical analyses on ferromanganese nodules and crusts, as well as some heavy minerals and phosphorites	https://www.ncmi.noaa.gov/access/metadata/landing-page/bin/iso?id=gov.noaa.nmms.mgg.geology:G01323 , last accessed: 7 January 2025	Over 140,000 element/oxide analyses	Global
GEOTRACES	Hydrographical and marine geochemical data	https://www.geotraces.org/ , last accessed: 7 January 2025	Data from 77 cruises and more than 800 hydrographic and geochemical parameters	Global
USGS	Geochemical information and related metadata from USGS research	https://www.usgs.gov/energy-and-minerals/mineral-resources-program/science/national-geochemical-database , last accessed: 16 July 2024	Extensive dataset	United States
BGS	Data on UK geology, boreholes, geomagnetism, groundwater, rocks, etc.	http://www.bgs.ac.uk/ , last accessed: 16 July 2024	Extensive dataset	United Kingdom
OZCHEM	Chemical compositions of rock, soil, and sediment samples	https://ecat.ga.gov.au/geonet/work/srv/ , last accessed: 16 July 2024	Extensive dataset	Australia
NOAA and MMS Marine Minerals Geochemical Database	Geochemical analyses on ferromanganese nodules and crusts, as well as some heavy minerals and phosphorites	https://www.ncmi.noaa.gov/access/metadata/landing-page/bin/iso?id=gov.noaa.nmms.mgg.geology:G01323, last accessed: 7 January 2025	Over 140,000 element/oxide analyses	Global
GEOTRACES	Hydrographical and marine geochemical data	https://www.geotraces.org/, last accessed: 7 January 2025	Data from 77 cruises and more than 800 hydrographic and geochemical parameters	Global

134

135

136

137

~~DM SED version 0.0.1 is presented in table (.csv) format. Dynamic versions of the most recent release can be found on Zenodo (<https://doi.org/10.5281/zenodo.13898366>, last accessed: 7 October 2024) (Lai et al., 2024), and a static copy of Version 0.0.1 is archived in the Geobiology [databasedata](#)~~

(<http://202.114.198.132/dmgeo-geobiology-portal/>, last accessed: 25 September 2024). In the following sections, we provide a brief overview of the database, information on the data sources and selection criteria, and a review of the definitions and decisions behind the metadata fields associated with each proxy measurement. We explore the spatial and temporal distribution trends of the compiled data and discuss future uses and limitations of the database.

2 Dataset overview

The DM-SED aims at collecting geochemical data from deep-time marine sediments. The database is primarily sourced from based on the SGP database, supplemented with additional ~~by~~ 34,874 newly compiled entries. The SGP contains a total of 82,578 entries, from which we selected 28,753 entries specifically related to marine sedimentary geochemical data, and is comprised of three parts: two parts from the U.S. Geological Survey (USGS), i.e. the National Geochemical Database (USGS NGDB, <https://mrdata.usgs.gov/ngdb/rock>, last accessed: 9 September 2024) and the Global Geochemical Database for Critical Metals in Black Shales project (USGS CMIBS, Granitto et al., 2017), with samples mainly from North America and Phanerozoic shales from various continents, respectively (Farrell et al., 2021). The third part comprises direct inputs by SGP members. The direct inputs in the Phase 1 SGP data release primarily focused on Neoproterozoic–Palaeozoic shales, although there are other lithologies and other time periods represented (Farrell et al., 2021). Our DM-SED database, built upon the SGP, includes a new compilation of 34,93834,874 entries from 433 studies, spanning approximately 3800 Ma and including entries~~entries from 433 literatures, covering a time range from approximately 3800 Ma to the present, and including entries~~ from North America, Europe, Asia, Africa, South America, Oceania, Pacific and Atlantic; thus~~thus~~ This~~ings~~ supplementing the temporal and spatial distribution gaps in the SGP database, and thereby creating a more comprehensive sedimentary marine geochemical database. The new compiled literatures span the time range from 1965 to 2023, with the number of papers per decade gradually increasing (Fig. 1). It should be noted that the top of the DM-SED version 0.0.1 data is the new compilation, and the bottom contains data imported from SGP.

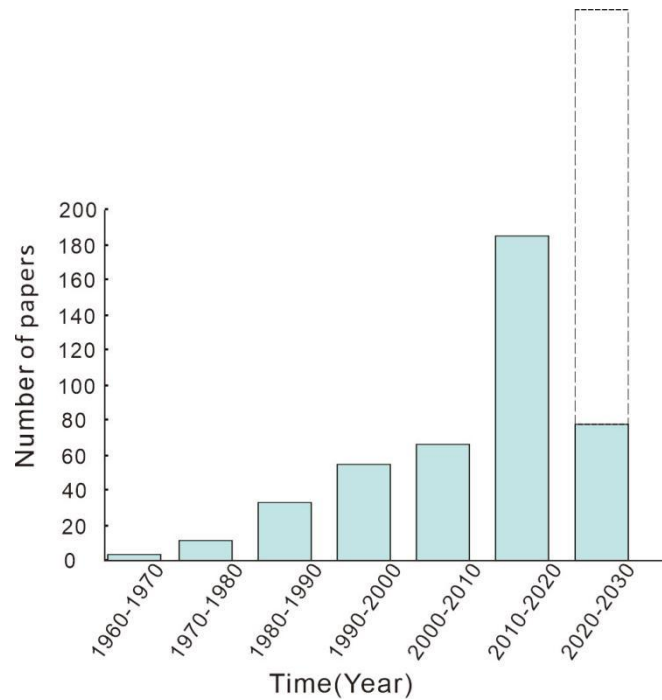
Table 2. Summary of data entries and points in the DM-SED.

	<u>Entries</u>	<u>Data points</u>
--	----------------	--------------------

<u>New compilation</u>	<u>34,874</u>	<u>1,454,400</u>
<u>SGP</u>	<u>28,753</u>	<u>1,067,855</u>
<u>DM-SED</u>	<u>63,627</u>	<u>2,522,255</u>

165

166



167

168 **Figure 1. The distribution of publication years for newly compiled literature (the dashed line denotes the**
 169 **predicted literature from 2023 to 2030).**

170

171 **Table 2. Summary of data entries and points in the DM-SED.**

	Entries	Data points
<u>New compilation</u>	<u>34,938</u><u>34,874</u>	<u>1,345,589</u><u>1,454,400</u>
<u>SGP</u>	<u>28,753</u>	<u>1,066,496</u><u>1,067,855</u>
<u>DM-SED</u>	<u>63,691</u><u>63,627</u>	<u>2,412,085</u><u>2,522,255</u>

172 The DM-SED database comprises **63,69163,627** entries with **2,412,0852,522,255** discrete data
 173 points (Table 2), each including location (SampleID, SampleName, SiteName, Region, Elevation,
 174 SampleDepth, ModLat, ModLon, PalaeoLat, PalaeoLon), age (Age, Period, Stage, Biozone),
 175 stratigraphic information (LithName, LithType, Formation, Facies), carbon element (total carbon (Total
 176 C), inorganic carbon (C_{inorg}), TOC, $\delta^{18}O_{carb}$, $\delta^{13}C_{Ker}$, $\delta^{13}C_{TOC}$, $\delta^{13}C_{carb}$, $\delta^{34}S_{CAS}$,

177 $\delta^{34}\text{S}_{\text{pyr}}$, $\delta^{15}\text{N}_{\text{total}}$, $\delta^{15}\text{N}_{\text{org}}$, in ‰), major element (P, Al, Si, Ti, Fe, Ca, Mg, Na, K, S, N, in wt%), trace
178 element (Ag, Ar, As, B, Ba, Be, Bi, Br, Cd, Ce, Co, Cr, Cs, Cu, Dy, Er, Eu, Ga, Gd, Ge, Hf, Hg, Ho, In,
179 La, Li, Lu, Mn, Mo, Nb, Nd, Ni, Pb, Pr, Rb, Re, Sb, Sc, Se, Sm, Sn, Sr, Ta, Tb, Te, Th, Tl, Tm, U, V,
180 W, Y, Yb, Zn, Zr, in ppm), [methodology \(TOC methods, Major elements methods, Trace elements](#)
181 [methods\)](#), and data sources (Reference, Project). The specific names and descriptions of each field in the
182 database are shown in Table 3. The standards and descriptions of isotope ratios in the database are shown
183 in Table 4.

184

185

186

187 **Table 3. Field names and descriptions.**

Field name	Description of field (units)
<i>Location fields</i>	
SampleID	Unique sample identification code
SampleName	Author denoted title for the sample (often non-unique)
SiteName	Name of the drill core site or section
Region	Country or ocean of the data collection site
Elevation	Distance between sampling location and sea level (m)
SampleDepth	Stratigraphic height or depth (m)
ModLat	Modern latitude of collection site rounded to two decimals; negative values indicate the Southern Hemisphere (decimal degrees)
ModLon	Modern longitude of the collection site rounded to two decimals; negative values indicate the Western Hemisphere (decimal degrees)
PalaeoLat	Palaeolatitude of collection site rounded to two decimals; negative values indicate the Southern Hemisphere (decimal degrees)
PalaeoLon	Palaeolongitude of the collection site rounded to two decimals; negative values indicate the Western Hemisphere (decimal degrees)
<i>Age fields</i>	
Age	Absolute Age, in reference to GTS2020 (Ma)
Period	The geologic period
Stage	The geologic stage (i.e. geochronologic age)
Biozone	Conodont, graptolite, ammonite biozone, etc
<i>Stratigraphy</i>	
LithName	Lithological name of the sample, as originally published
LithType	Lithology type of sample (e.g. carbonate, siliciclastic)
Formation	Geologic formation name
Facies	Depositional environment (e.g. mid-shelf, ramp)
<i>Proxy fields</i>	

Carbon	The content of carbon, including Total C, C _{inorg} , TOC, rounded to two decimals (wt%)
Isotopes	The isotope value, rounded to two decimals (‰)
Major elements	The content of major elements such as P, Al, and Si, rounded to two decimals (wt%)
Trace elements	The content of trace elements such as Ag, Ar, As, B, and Ba, rounded to two decimals (ppm)
<u>Methodology</u>	
TOC content-methods	A brief description of the testing methods for TOC
Major elements methods	A brief description of the testing methods for major elements
Trace elements methods	A brief description of the testing methods for trace elements
<u>Data sources</u>	
Reference	Data sources, including published literature or other databases
Project	Two parts: new compilation and SGP

188

189

190

191

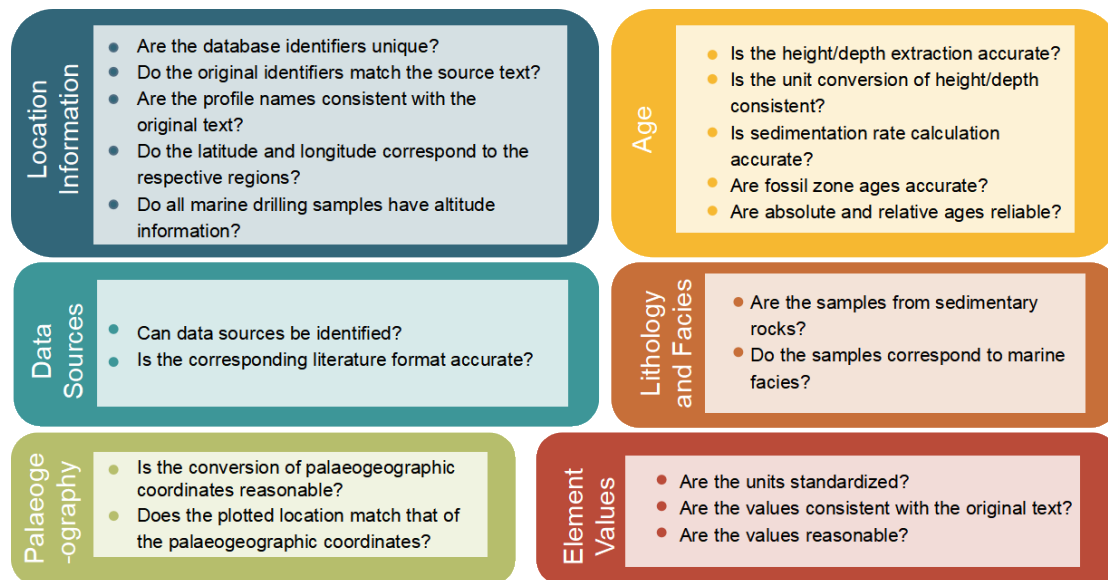
Table 4. Standards and descriptions of isotope ratios in the DM-SED.

Symbol	Standard	Description
$\delta^{18}\text{O}_{\text{carb}}$	Vienna Pee Dee Belemnite (VPDB)	Oxygen isotope ratio of carbonate minerals, used in palaeoclimate studies.
$\delta^{13}\text{C}_{\text{Ker}}$	VPDB	Carbon isotope ratio of kerogen, used to study the source and depositional environment of organic matter.
$\delta^{13}\text{C}_{\text{TOC}}$	VPDB	Carbon isotope ratio of total organic carbon, used to analyse the source of organic matter and biogeochemical cycles in sediments.
$\delta^{13}\text{C}_{\text{carb}}$	VPDB	Carbon isotope ratio of carbonate minerals, used in palaeoclimate and carbon cycle research.
$\delta^{34}\text{S}_{\text{CAS}}$	Vienna Canyon Diablo Troilite (VCDT)	Sulfur isotope ratio of carbonate-associated sulfate, used to study the sulfur cycle and redox conditions.
$\delta^{34}\text{S}_{\text{pyr}}$	VCDT	Sulfur isotope ratio of pyrite, typically used to investigate the sulfur cycle and redox conditions in ancient oceans.
$\delta^{15}\text{N}_{\text{total}}$	Atmospheric Nitrogen (air N ₂)	Nitrogen isotope ratio of total nitrogen, used to study the nitrogen cycle and nutrient sources.
$\delta^{15}\text{N}_{\text{org}}$	air N ₂	Nitrogen isotope ratio of organic nitrogen, often used to analyse the source of organic matter and the nitrogen cycle.

192

193 3 Dataset screening and processing

194 This section details the screening and processing criteria for sample location, age, lithology and facies,
195 specific geochemical values, and data source information (Fig. 2).



196
197 **Figure 2. The data filtering and processing criteria for DM-SED.**

198 For sample location, the [datasetbase](#) includes SampleID, SampleName, SiteName, Region,
199 Elevation, SampleDepth, ModLat, ModLon, PalaeoLat, and PalaeoLon. A unique SampleID is assigned
200 to each sample in the DM-SED. The SampleName corresponds to the identifier given in each referenced
201 publication, facilitating cross-referencing with the original data. The SiteName includes well name or
202 outcrop information, representing the smallest unit of location information. The Region indicates the
203 country or ocean area where the sample has been collected and represents a broader geographical range.
204 The Elevation data are mainly related to samples from the Deep Sea Drilling Project (DSDP) and the
205 Ocean Drilling Program (ODP) collected from post-Cretaceous sediments and indicate whether the
206 samples originate from deep or shallow marine environments. SampleDepth refers to the relative position
207 (in metres) of the sample within the well or outcrop, which is crucial for calculating sample age. In some
208 publications, specific heights are not provided directly but are given as relative heights through figures.
209 We manually extracted these heights using WebPlotDigitizer, rounding to two decimal places (Drevon
210 et al., 2017). For publications in which heights are expressed in feet or centimetres, we converted the
211 units to metres. Modern latitude and longitude (ModLat and ModLon) information are the most precise
212 location data. Although some publications provide exact coordinates, many offer only section names (i.e.
213 SiteName) and regions or merely a map marking the location of the section. For publications providing

214 section names, we determined accurate coordinates by consulting other studies carried out in the same
215 section. For those providing only a map marking the location of the section, we used Google Maps to
216 estimate relative coordinates. To ensure consistency, we recorded sample coordinates in decimal degrees,
217 rounded to two decimal places, with positive values indicating north latitude and east longitude and
218 negative values indicating south latitude and west longitude. And the coordinate reference system is
219 WGS 84 (World Geodetic System 1984). For palaeo-coordinates, we reconstructed palaeo-latitude and
220 palaeo-longitude (PalaeoLat, and PalaeoLon) using the sample age and modern coordinates, employing
221 the PointTracker v7 rotation files from the PALEOMAP project, which are based on current geographic
222 reference data and global tectonic history models (Scotese, 2008). It is important to note that we only
223 generated palaeogeographic locations for samples from the Phanerozoic, as the geological records from
224 this time are more complete and abundant compared to those from the Precambrian, making the
225 reconstruction of geographic features (such as ancient oceans, mountains, plains, etc.) relatively more
226 reliable and accurate (Scotese and Wright 2018). We plotted the sample points on palaeogeographic maps
227 based on Scotese's data using QGIS 3.16 (Scotese and Wright 2018).

228 To assign specific ages to each sample in the database, we assumed a constant sedimentation
229 rate within the same formation or group of section. If the original studies provided numerical ages for
230 two or more samples, we calculated the precise age for each sample based on the sedimentation rate and
231 assigned it accordingly. If absolute ages were not provided in the original literature, we assigned
232 approximate ages based on corresponding fossil zones or the general age of the same lithostratigraphic
233 unit in the same region (Farrell et al., 2021; Judd et al., 2022). For samples with completely missing
234 height information in the original text, we assigned the same age to all samples within the section based
235 on lithostratigraphic information. However, the primary age constraints for these samples (mainly from
236 USGS NGDB and USGS CMIBS) remain derived from SGP age calls.~~For samples with completely~~
237 ~~missing height information in the original text, we assigned the same age to all samples within the section~~
238 ~~based on lithostratigraphic information (mainly samples from USGS NGDB and USGS CMIBS).~~ Once
239 each sample had a specific age, we assigned it to a specific Period and Stage according to its age. We
240 attempted to incorporate the most recent age models; however, due to the extensive size of the data
241 compilation, it was not feasible to update all of them. All ages were based on the timescale provided by
242 the Geologic Time Scale 2020 (Gradstein et al., 2020). Although GTS 2020 is accurate, readers are
243 advised to consult the incremental updates of the International Chronostratigraphic Chart (ICS) for the

244 most accurate stratigraphic intervals

245 .

246 For lithology and facies, the lithologies include shale, mudstone, sandstone, limestone,
247 ~~dolostone~~~~dolomite~~, and others. We classified these into two ~~major~~ types of rocks: siliciclastic
248 sedimentary rocks (88.7%) and carbonate rocks (11.3%). For outcrop sections, the lithostratigraphic unit
249 was generally available; however, ~~for data from marine drilling sites~~~~for marine drilling data~~, there was
250 ~~often~~~~were~~ no corresponding lithostratigraphic unit information~~group~~ ~~names~~. Regarding facies
251 classification, before the Cretaceous, the primary depositional environment was marine settings on
252 continental crust, including specific facies such as ~~tidal flats~~, inner shelves, outer shelves, and basinal.
253 ~~However, after the Cretaceous, with most samples coming from DSDP and ODP, deep ocean~~
254 ~~depositional environments emerged.~~However, after the Cretaceous, with most samples coming from the
255 DSDP and ODP, shallow marine depositional environments still existed and were sampled, but deep-sea
256 pelagic settings began to be sampled as well~~emerge~~.

257 For specific geochemical values in the DM-SED database, we standardized the units, converting
258 oxides to elements (e.g. P (ppm) to P (wt%), P₂O₅ (wt%) to P (wt%)). If a sample was analysed multiple
259 times, we averaged the value. For literature before 2000, some data were preserved as images, requiring
260 manual extraction of values, and some images were slightly blurry, potentially leading to minor human
261 error. We excluded data that were beyond detection limits (e.g. the trace element content is too low and
262 the value provided in the text represents the minimum detection limit) or unreasonable (e.g. negative
263 values for major and trace elements).

264 For the ~~testing methods of the data~~geochemical methodology, we briefly documented them based
265 on the descriptions in the original text, focusing primarily on the testing methods and instrument models
266 used for TOC, major elements, and trace elements. Methods for stable isotopes were not documented,
267 as the testing methods vary for different isotopes, and due to the limited amount of isotope data, recording
268 them holds little significance.

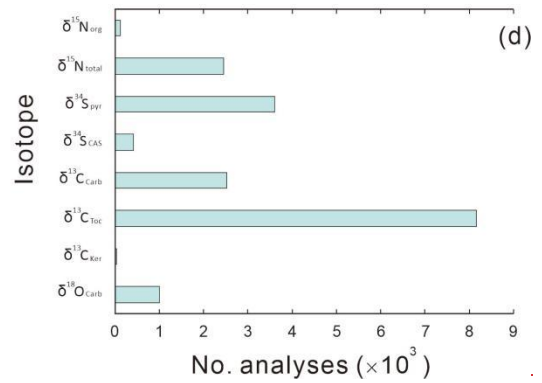
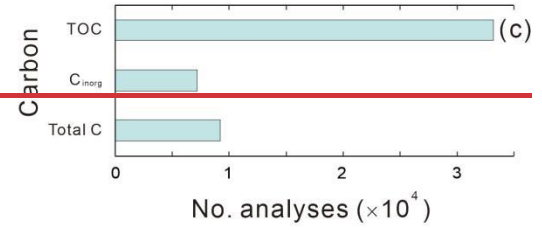
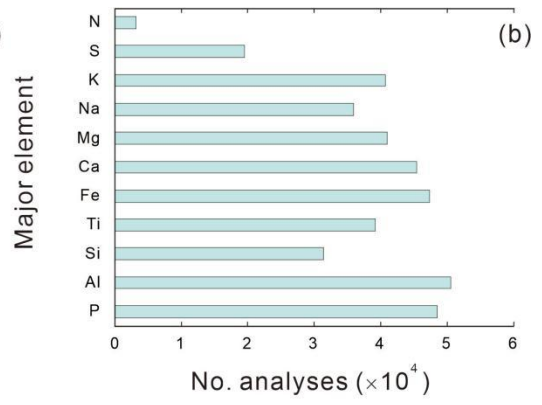
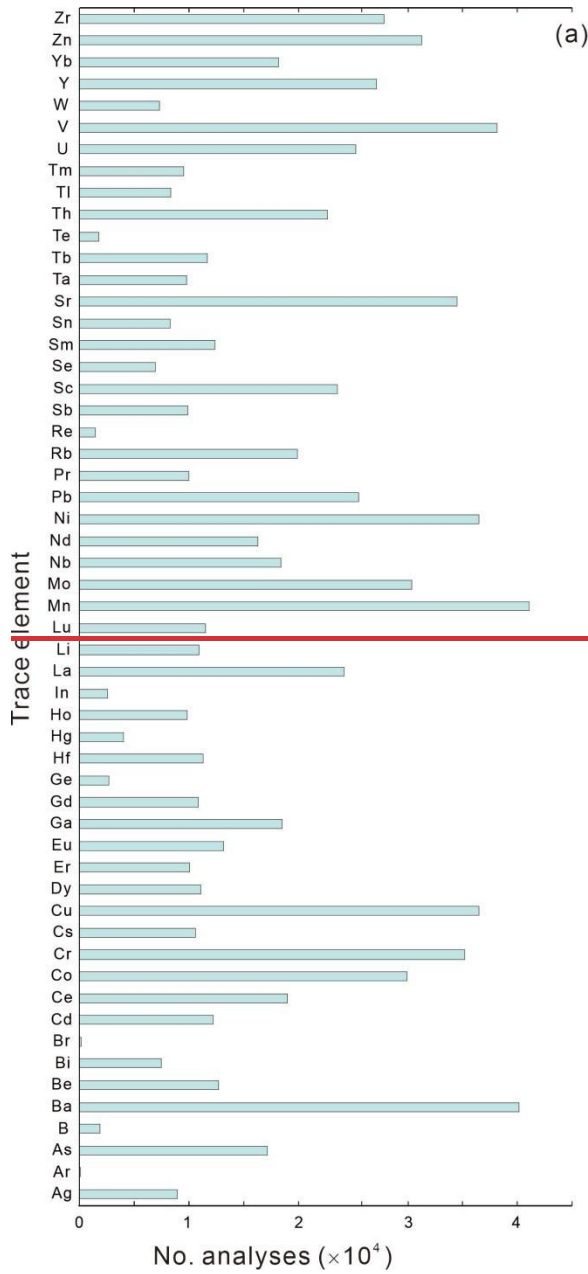
269 Regarding data sources, we ensured that each corresponding reference was collected and listed in
270 full citation format, including authors, title, publication date, journal, page numbers, and DOI. Most data
271 in the SGP database came directly from USGS NGDB and USGS CMIBS, without corresponding
272 literature sources, so we marked them individually. The entire database for this Project was divided into
273 two parts: new compilation and SGP~~And the project includes two parts: new compilation and SGP~~. We

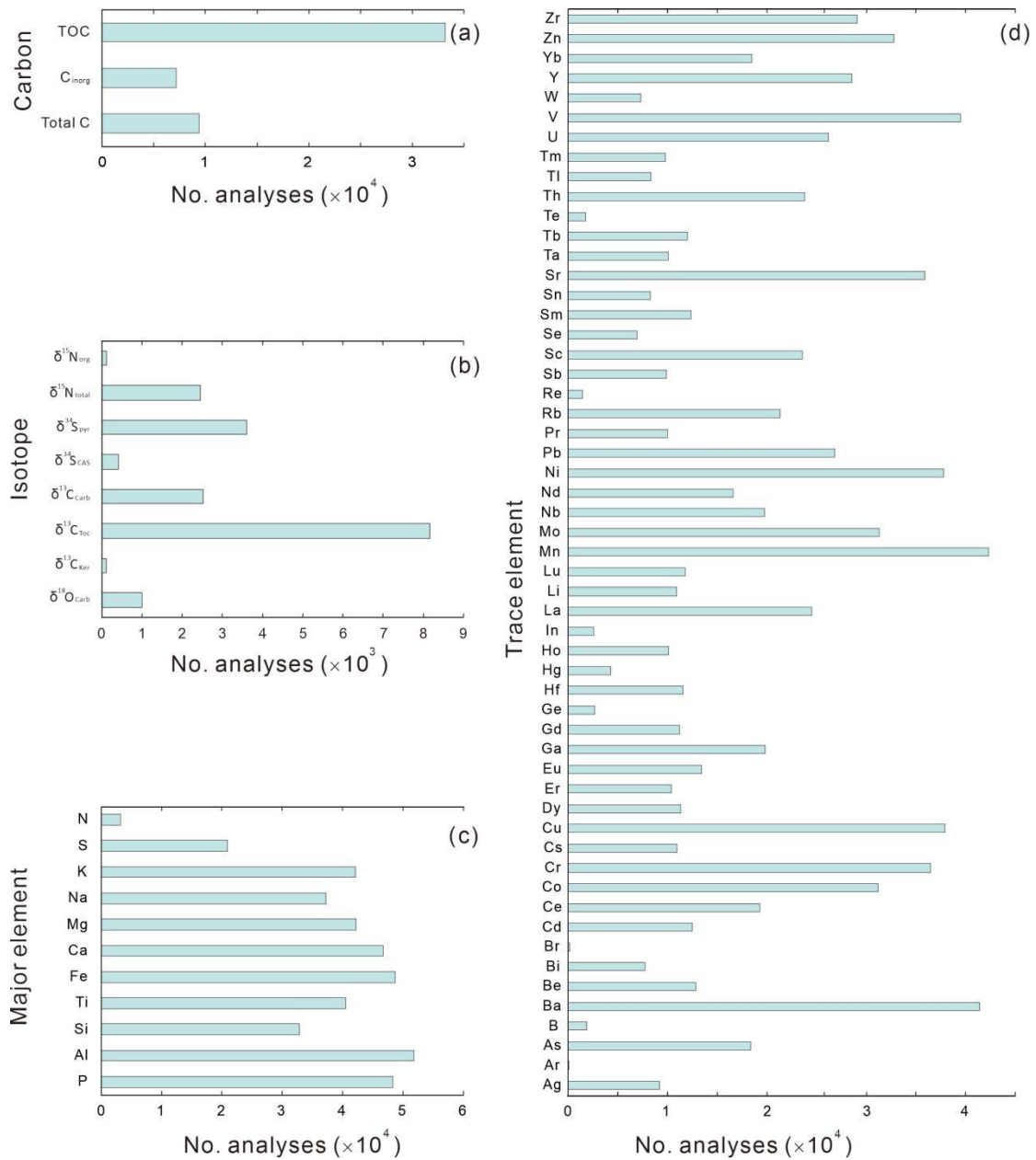
274 used keyword searches in Google Scholar to identify missing references and made efforts to target
275 literature for data-scarce regions (e.g. South America) and time intervals (e.g. Silurian, Jurassic).

276 **4 Data distribution**

277 The elemental data content distribution for the entire database is shown in Fig. 3. Overall, major elements
278 have the highest data quantity, followed by trace elements and carbon elements, with isotope data having
279 the lowest quantity. Among the major elements, N has the fewest entries, with 3,164 records, whereas
280 the other major elements all have more than 10,000 entries. Al has the highest quantity, with 501,568,906
281 records. Among trace elements, Mn has the largest record (412,058,499 records), followed by Ba
282 (401,163,470 records). Ar and Br have the fewest records, with 9 and 16,276 records, respectively. Other
283 elements such as Ag, B, Bi, Ge, Hg, ~~Ho~~, In, ~~Pr~~, Re, ~~Sb~~, Se, Sn, ~~Ta~~, Te, Tl, Tm, and W have data quantities
284 ranging from 1,000 to 10,000. Elements such as As, Be, Cd, Ce, Co, Cr, Cs, Cu, Dy, Er, Eu, Ga, Gd, Hf,
285 ~~Ho~~, La, Li, Lu, Mo, Nb, Nd, Ni, Pb, ~~Pr~~, Rb, ~~Sb~~, Sc, Sm, Sr, ~~Ta~~, Tb, Th, U, V, Y, Yb, Zn, and Zr all have
286 more than 10,000 records each. For carbon elements, TOC has the largest record (32,9046 entries),
287 followed by Total C (9,386 entries), while C_{inorg} has the lowest record (7,215 entries)~~For carbon elements,~~
288 ~~TOC has the most records, with 33,216 entries, followed by Total C with 9,201 entries. C_{inorg} has the~~
289 ~~fewest records, with 7,194 entries.~~ Isotope data are overall less abundant, with none exceeding 10,000
290 entries; the most abundant is $\delta^{13}\text{C}_{\text{TOC}}$, with 8,166 records, and the least abundant is $\delta^{13}\text{C}_{\text{Ker}}$, with only
291 112,29 records.

292





294

295 **Figure 3. Histogram distribution of different subsets. (a) Trace elements, (b) Major elements, (c) Carbon**
 296 **elements, (d) Isotopes, (e) Major elements, (f) Trace elements.**

297

298

299

300

301

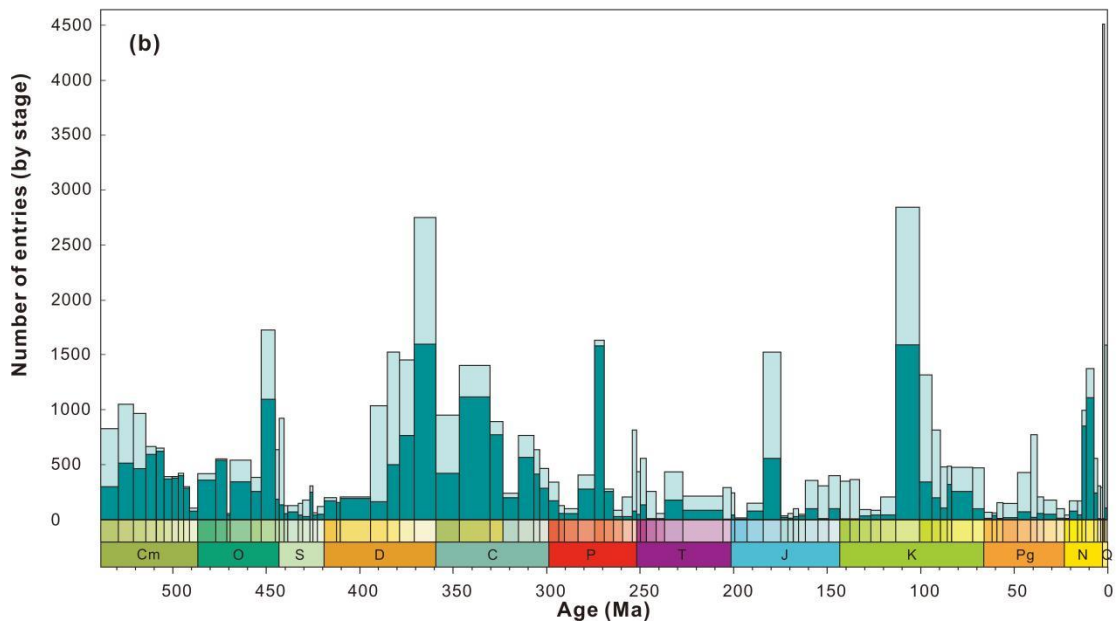
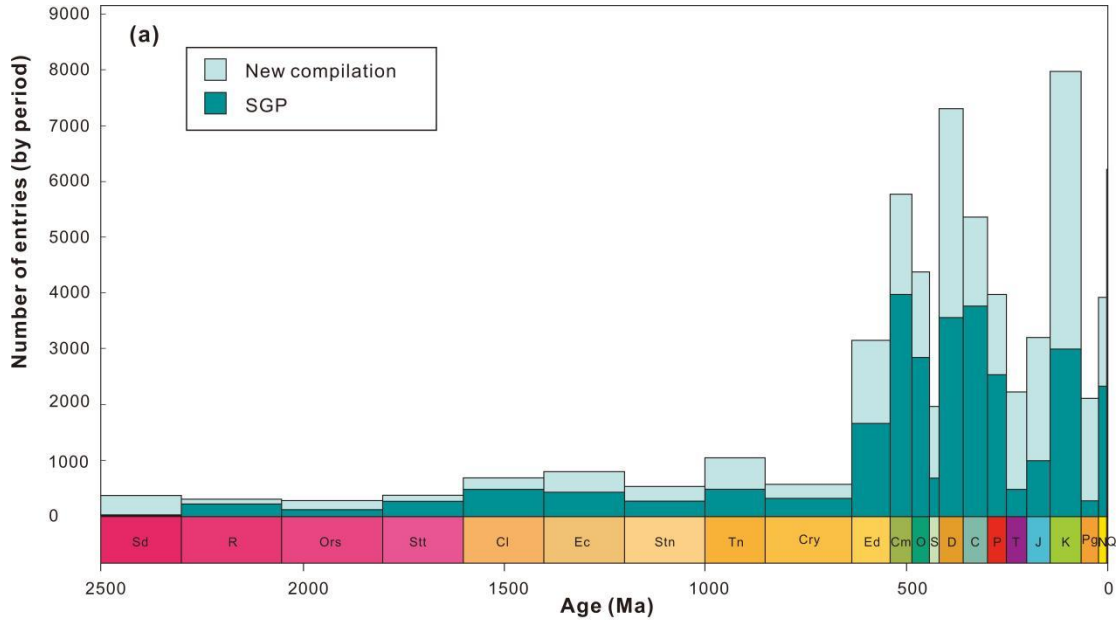
302

303

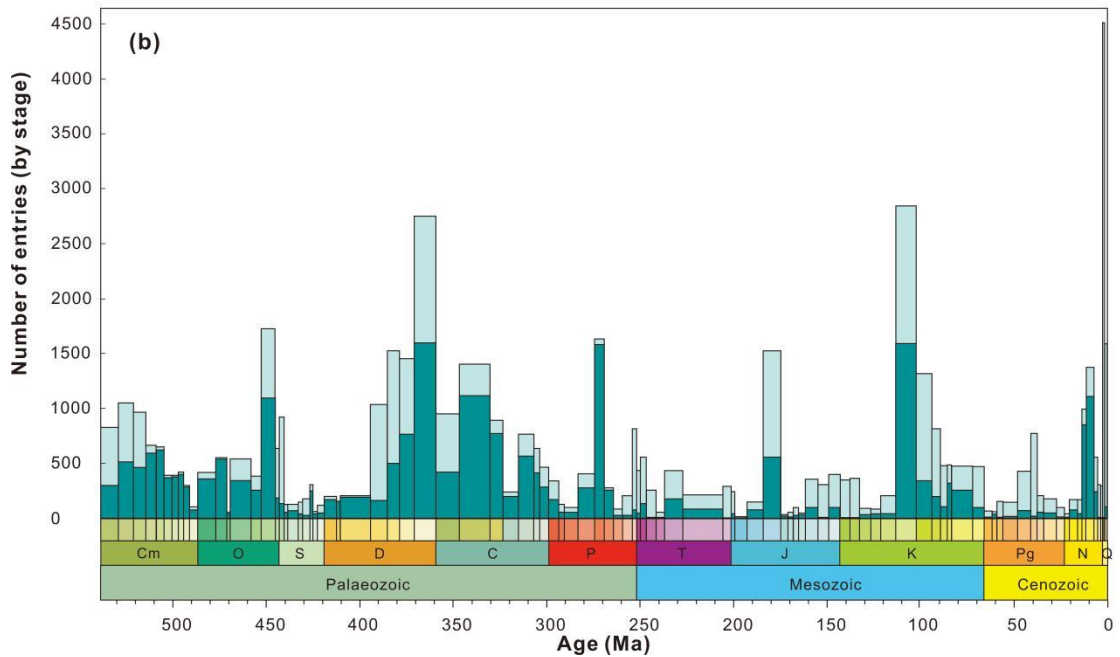
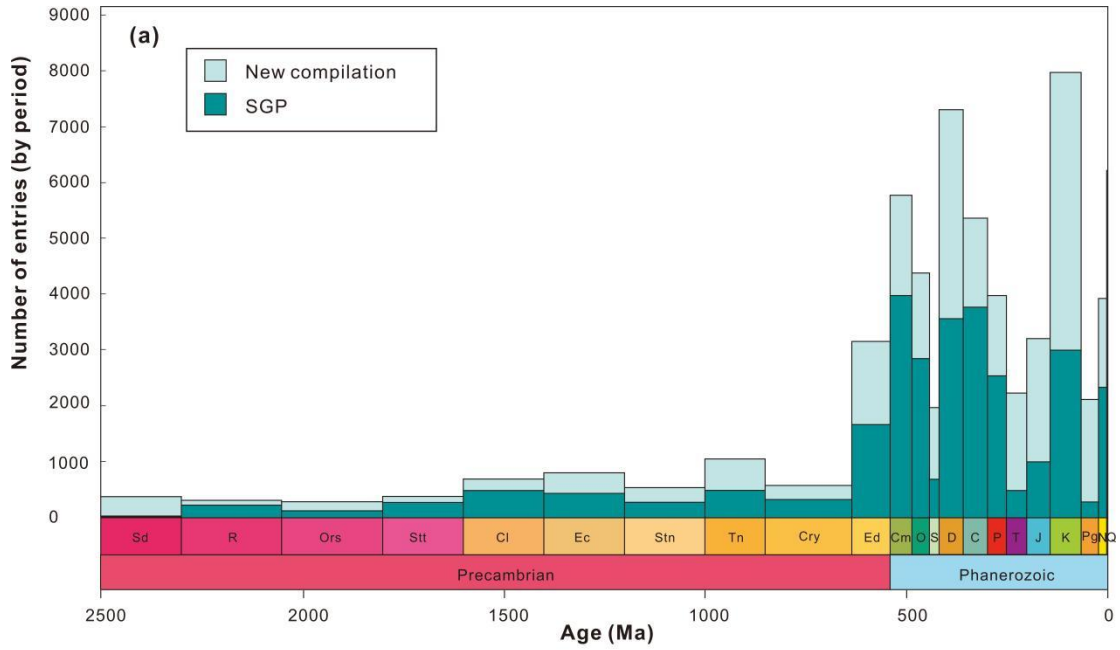
The temporal trend of data density in the entire database, shown in Fig. 4a, indicates that the data are primarily distributed in the Phanerozoic Eon, which accounts for 85% of the entire database. Within the Phanerozoic From this, the Cenozoic Era accounts for 19% of the database, the Mesozoic Era accounts for 21%, and the Palaeozoic Era accounts for 45%. Precambrian data account for only 15% of the entire database. The SGP data are most concentrated in the Palaeozoic Era, in which they make up 27% of the total database, with the new compiled data contributing only 18%. In other eras, the new compiled data outnumber the SGP data: 4% versus 15% in the Cenozoic, 7% versus 14% in the Mesozoic, and 7%

304 versus 8% in the Precambrian. This is mainly the case because the SGP data in the first phase were
 305 primarily from the Neoproterozoic and Palaeozoic eras (Farrell et al., 2021).

306



307



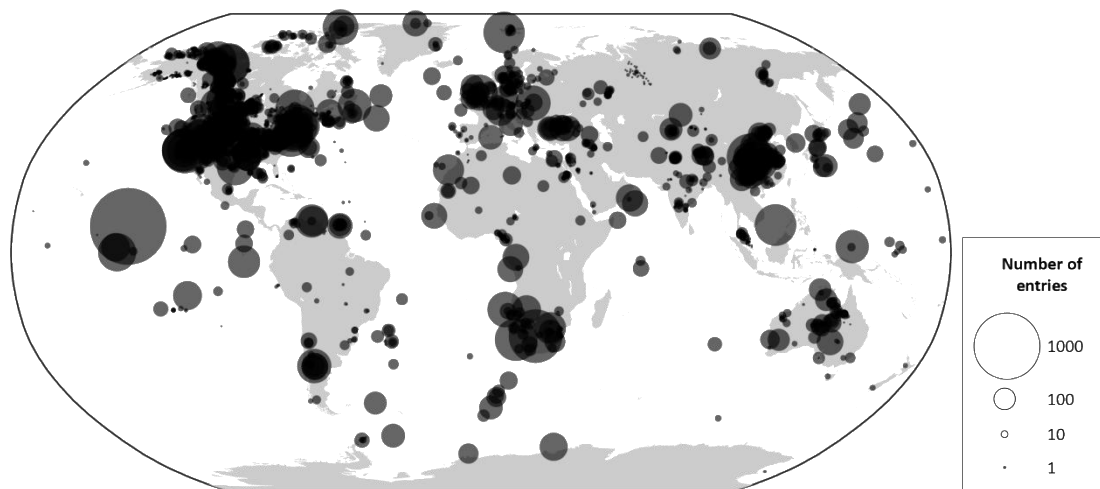
308

309 Figure 4. The age distribution of samples in the database. (a) Age distribution of samples (excluding a small
 310 number of samples with ages >2500 Ma from the figure, a total of 12958 samples). (b) Age distribution of
 311 Phanerozoic samples at the stage level. Sd, Siderian; R, Rhvagian; Sd, Siderian; Ors, Orosirian; Stt,
 312 Statherian; Cl, Calymmian; Ec, Ectasian; Stn, Stenian; Tn, Tonian; Cry, Cryogenian; Ed, Ediacaran; Cm,
 313 Cambrian; O, Ordovician; S, Silurian; D, Devonian; C, Carboniferous; P, Permian; T, Triassic; J, Jurassic;
 314 K, Cretaceous; Pg, Paleogene; N, Neogene; Q, Quaternary.

315

316

317 For the distribution of sample ages within the Phanerozoic, we divided the samples by stage, as
318 shown in Fig. 4b. For the Quaternary Period, due to its short duration, ~~data were not subdivided by Stage,~~
319 ~~but only into Holocene and Pleistocene.~~the data were not subdivided by Stage but were instead divided
320 into the Holocene and Pleistocene Series. Data distribution is not uniform, with the highest concentration
321 in the Quaternary Period. These data mainly come from DSDP and ODP, which are characterised by a
322 high number of core samples and high resolution. There are fewer data for the Upper Permian, Lower
323 Triassic, and Lower to Middle Jurassic, possibly because of the existence of Pangaea at that time, which
324 reduced the area of continental margins and inhibited marine transgressions, resulting in fewer preserved
325 marine environments in comparison to those of other geological periods (Mackenzie and Pigott, 1981;
326 Walker et al., 2002). The distribution of sample quantities in other periods fluctuates, often corresponding
327 to periods of significant research interest, such as the end-Ordovician, end-Devonian, end-Permian, Early
328 Jurassic Toarcian and Early Cretaceous Albian, which had peaks in sample numbers due to their
329 association with major mass extinction events and oceanic anoxic events (Fan et al., 2020).

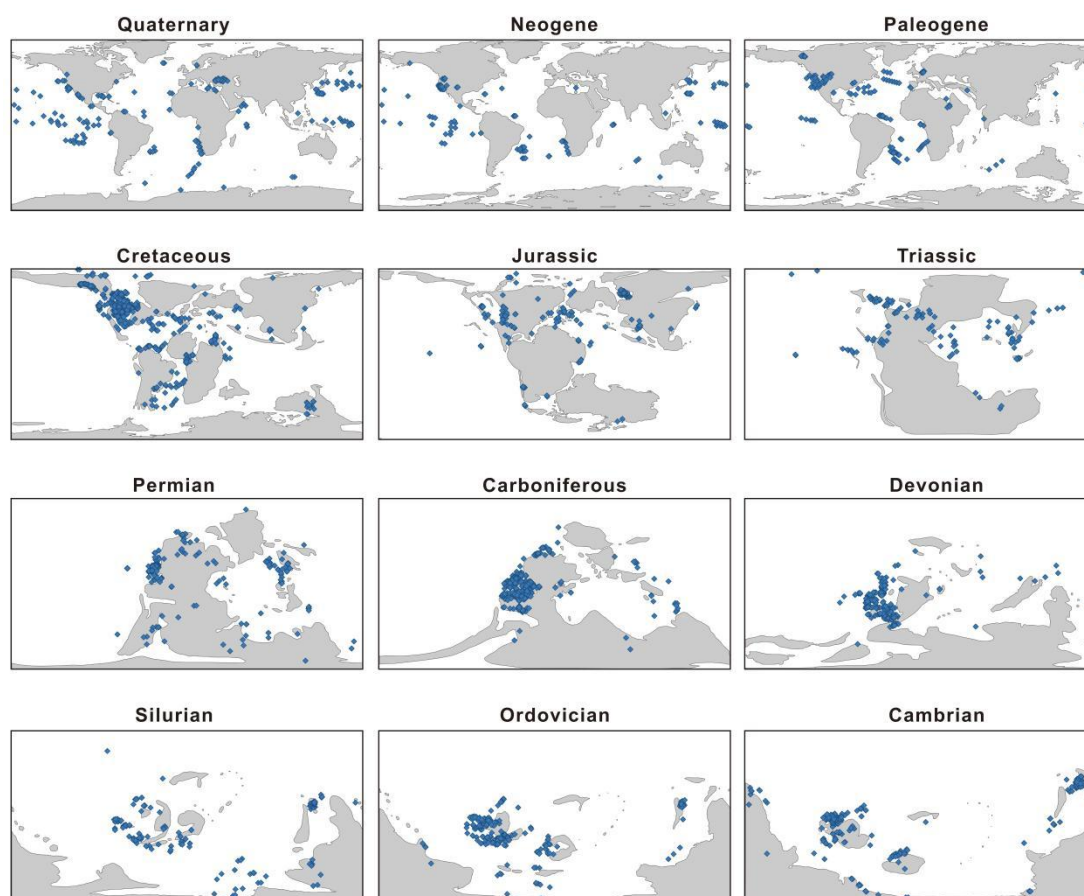


330

331 **Figure 5. Bubble chart of modern geographical distribution and sample quantities in the database.**

332 In terms of spatial trends, the spatial distribution of sampling points in the DM-SED database is
333 inherently uneven, both in modern and palaeogeographic locations. Modern locations are primarily
334 concentrated in North America, Europe, South Africa, and China (Fig. 5). When modern coordinates are
335 converted to palaeogeographic coordinates and projected onto palaeogeographic maps, Cambrian to
336 Jurassic data come predominantly from continental margin environments, as ~~oceanic crust plates~~
337 ~~subductingsubduction of oceanic crust~~ before the Cretaceous ~~resulted in~~~~led to~~ preservation of very few
338 deep-sea environments (Fig. 6). Cambrian and Ordovician data are distributed mainly on the Laurentia,

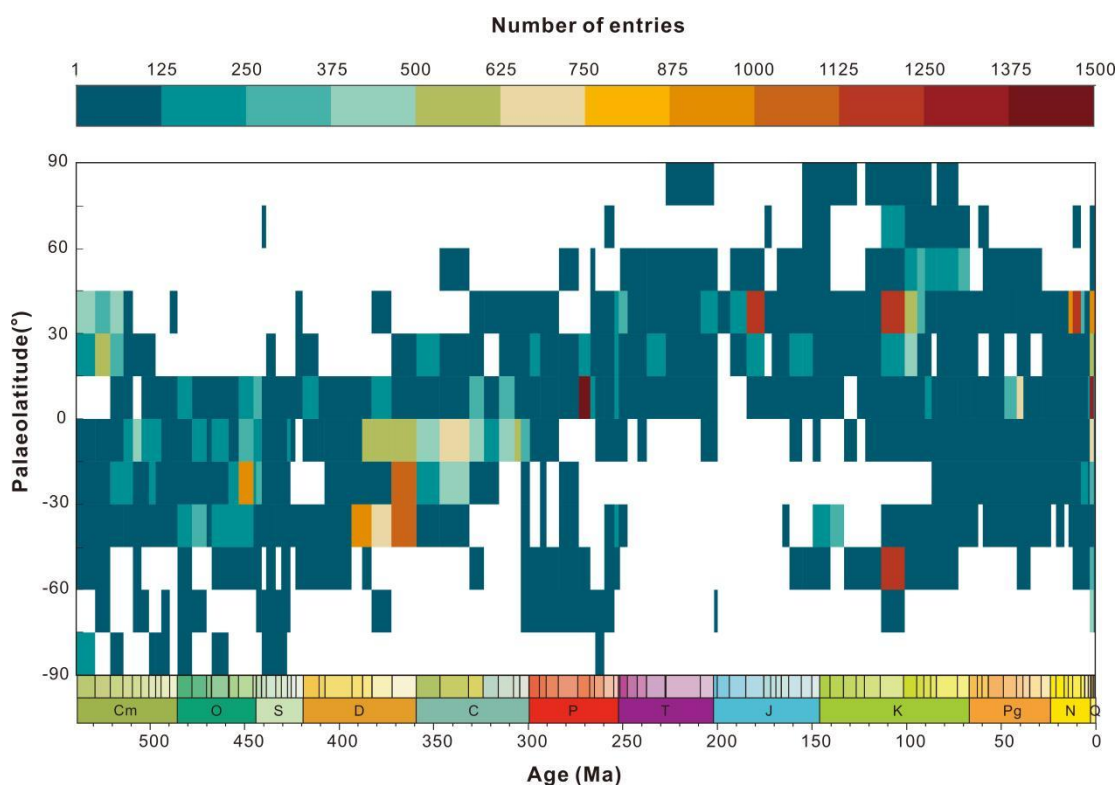
339 Baltica, and South China plates, with a few along the Gondwana margin. Silurian data occur mainly on
 340 Laurentia, South China, and eastern Gondwana~~right side of Gondwana~~. Devonian and Carboniferous
 341 data are primarily on the Laurussia plate, with sparse distribution in South China and Gondwana. Permian
 342 and Triassic data are mainly on the Laurussia and South China plates, with sparse distribution in
 343 Gondwana. Jurassic data are primarily on the North American, European ~~shelf~~, with sparse distribution
 344 on other plates. From the Cretaceous to the Quaternary, sample locations, dominated by data from the
 345 DSDP, ODP, and USGS NGDB projects, are mainly located in the deep oceans and North America.



346
 347 **Figure 6. The palaeogeographic distribution of sample sites in the DM-SED.**

348 When averaging all Phanerozoic data by stage and spatially averaging them into 15° palaeolatitude
 349 bins (Fig. 7), Palaeozoic data records are mainly biased toward tropical regions. Cambrian data are
 350 concentrated between 15° S and 30° N, Ordovician to Carboniferous data are concentrated between 45°
 351 S and 15° N, and Permian data are concentrated between 0° N and 30° N, with data mainly fluctuating
 352 around the equator. As continents migrated northward through the Mesozoic and into the Cenozoic,
 353 records began to show bias toward mid-latitudes in the Northern Hemisphere. From the Triassic to the
 354 Cretaceous, data are mainly concentrated between 0° N and 60° N. And Paleogene to Quaternary data

355 [are concentrated between 45° S and 45° N.](#)



356

357 **Figure 7. The spatiotemporal distributions of sample quantities (categorized temporally by stage and spatially**
358 **by palaeolatitude intervals of 15°).**

359

360 5 Usage instructions

361 The ultimate goal of the DM-SED database is to provide the geoscience community with a valuable
362 resource of knowledge and geographic information. By deriving meaningful conclusions from a large
363 marine sediment geochemistry [database](#), we aim to enhance our understanding of Earth's
364 environmental changes over time and space. All entries in DM-SED contain the source of original proxy
365 values, ensuring traceability between DM-SED and the original datasets from which the data were
366 extracted.

367 However, our database has some limitations. The criteria for age determination, relying variously
368 on fossil zones and lithostratigraphic unit information, are not entirely uniform. Some age determinations
369 are still coarse, with samples from a single section [all](#) assigned the same age. Additionally, the data
370 quantity for some elements is still low. ~~The testing methods for elements are not annotated, and there~~
371 may be significant differences in methodological precision between older and newer literature. Currently,

372 these issues remain largely unresolved. Despite our best efforts to identify data from the literature and
373 process quality control for each entry, the sheer volume of data in DM-SED means that some errors or
374 omissions are inevitable. Prompt corrections and continuous updates are expected to ensure the
375 credibility of this ~~dataset~~base.

376 Finally, it is important to recognize that DM-SED merely compiles these various datasets and
377 cannot impose any requirements on their generation. When using the data (and where practicable), we
378 recommend citing both DM-SED and the original data sources to ensure proper attribution.

379

380 **6 Data availability**

381 Version controlled releases of the DM-SED can be found on Zenodo
382 (~~<https://doi.org/10.5281/zenodo.13898366>~~<https://doi.org/10.5281/zenodo.14771859>, last accessed: 30
383 January 2025~~last accessed: 7 October 2024~~) (~~Lai et al., 2024~~Lai et al., 2025). A static copy of DM-SED
384 version 0.0.1 is archived in the Geobiology ~~database~~data ([http://202.114.198.132/dmgeo-geobiology-](http://202.114.198.132/dmgeo-geobiology-portal/)
385 [portal/](http://202.114.198.132/dmgeo-geobiology-portal/), last accessed: 25 September 2024). We plan to supplement and improve the ~~dataset~~base
386 continuously and hope to collaborate with existing compilation authors to assist in adding new content.

387

388 **7 Code availability**

389 The software tools used in this study are available at the following links: WebPlotDigitizer can be
390 downloaded from <https://github.com/automeris-io/WebPlotDigitizer/releases> (last accessed: 20 July
391 2024); the PointTracker v7 tool can be found at <http://www.paleogis.com> (last accessed: 20 July 2024);
392 QGIS 3.16 can be downloaded from the <https://qgis.org/project/overview/> (last accessed: 20 July 2024).

393

394 **Author contributions.** Jiankang Lai: Writing – original draft, Visualization, Data collection,
395 Investigation. Haijun Song: Writing – review & editing, Supervision, Investigation, Funding acquisition.
396 Daoliang Chu: Writing– review & editing, Investigation. Jacopo Dal Corso: Writing– review & editing,
397 Investigation. Erik A. Sperling: Writing– review & editing, Investigation.

398 Yuyang Wu: Writing– review & editing, Supervision, Investigation, Data collection. Xiaokang Liu:

399 Writing– review & editing, Investigation. Lai Wei: Writing– review & editing, Data collection,
400 Investigation. Mingtao Li: Writing– review & editing, Investigation. Hanchen Song: Writing– review &
401 editing, Investigation. Yong Du: Writing– review & editing, Investigation. Enhao Jia: Writing– review
402 & editing, Investigation. Yan Feng: Writing– review & editing, Investigation. Huyue Song: Writing–
403 review & editing, Investigation. Wenchao Yu: Writing– review & editing, Investigation. Qingzhong
404 Liang: Writing– review & editing, Investigation. Xinchuan Li: Writing– review & editing, Investigation.
405 Hong Yao: Writing– review & editing, Investigation.

406

407 **Competing interests.** The authors declare that they have no conflicts of interest.

408

409 **Acknowledgements.**

410 ~~We thank Xiang Shu for the discussions on analytical methods. This paper benefited greatly from~~
411 ~~comments from xxx anonymous reviewers. This paper benefited greatly from comments from Thierry~~
412 ~~Adatte and an anonymous reviewer and reviewer Thierry Adatte. We also thank Jan Peter (Research~~
413 ~~Scientist, Geological Survey of Canada) for providing his literature data.~~

414

415 **Funding:**

416 This study was supported by the National Natural Science Foundation of China grant 42325202, the State
417 Key R&D Project of China (2023YFF0804000), 111 Project grant B08030, ~~and~~ Natural Science
418 Foundation of Hubei (2023AFA006), and Graduate Student Project from the Hubei Research Center for
419 Basic Disciplines of Earth Sciences (NO. HRCES-202413). E.A.S. is supported by United States
420 National Science Foundation grant EAR-2143164.

421

422 **REFERENCES**

423 Algeo, T. J. and Liu, J.: A re-assessment of elemental proxies for paleoredox analysis, Chem. Geol., 540,
424 119549, <https://doi.org/10.1016/j.chemgeo.2020.119549>, 2020.

425 Drevon, D., Fursa, S. R., and Malcolm, A. L.: Intercoder Reliability and Validity of WebPlotDigitizer in
426 Extracting Graphed Data, Behav. Modif., 41, 323-339, <https://doi.org/10.1177/0145445516673998>,

427 2017.

428 FAIR-: FAIR Play in geoscience data, *Nat. Geosci.*, 12, 961, [https://doi.org/10.1038/s41561-019-0506-](https://doi.org/10.1038/s41561-019-0506-4)
429 4, 2019.

430 Fan, J., Shen, S., Erwin, D. H., Sadler, P. M., MacLeod, N., Cheng, Q., Hou, X., Yang, J., Wang, X.,
431 Wang, Y., Zhang, H., Chen, X., Li, G., Zhang, Y., Shi, Y., Yuan, D., Chen, Q., Zhang, L., Li, C.,
432 and Zhao, Y.: A high-resolution summary of Cambrian to Early Triassic marine invertebrate
433 biodiversity, *Science*, 367, 272-277, <https://doi.org/10.1126/science.aax4953>, 2020.

434 Farrell, U. C., Samawi, R., Anjanappa, S., Klykov, R., Adeboye, O. O., Agic, H., Ahm, A. C., Boag, T.
435 H., Bowyer, F., Brocks, J. J., Brunoir, T. N., Canfield, D. E., Chen, X., Cheng, M., Clarkson, M.
436 O., Cole, D. B., Cordie, D. R., Crockford, P. W., Cui, H., Dahl, T. W., Mouro, L. D., Dewing, K.,
437 Dornbos, S. Q., Drabon, N., Dumoulin, J. A., Emmings, J. F., Endriga, C. R., Fraser, T. A., Gaines,
438 R. R., Gaschnig, R. M., Gibson, T. M., Gilleaudeau, G. J., Gill, B. C., Goldberg, K., Guilbaud, R.,
439 Halverson, G. P., Hammarlund, E. U., Hantsoo, K. G., Henderson, M. A., Hodgskiss, M. S. W.,
440 Horner, T. J., Husson, J. M., Johnson, B., Kabanov, P., Brenhin Keller, C., Kimmig, J., Kipp, M.
441 A., Knoll, A. H., Kreitsmann, T., Kunzmann, M., Kurzweil, F., LeRoy, M. A., Li, C., Lipp, A. G.,
442 Loydell, D. K., Lu, X., Macdonald, F. A., Magnall, J. M., Mand, K., Mehra, A., Melchin, M. J.,
443 Miller, A. J., Mills, N. T., Mwinde, C. N., O'Connell, B., Och, L. M., Ossa Ossa, F., Pages, A.,
444 Paiste, K., Partin, C. A., Peters, S. E., Petrov, P., Playter, T. L., Plaza-Torres, S., Porter, S. M.,
445 Poulton, S. W., Pruss, S. B., Richoz, S., Ritzer, S. R., Rooney, A. D., Sahoo, S. K., Schoepfer, S.
446 D., Sclafani, J. A., Shen, Y., Shorttle, O., Slotznick, S. P., Smith, E. F., Spinks, S., Stockey, R. G.,
447 Strauss, J. V., Stueken, E. E., Tecklenburg, S., Thomson, D., Tosca, N. J., Uhlein, G. J., Vizcaino,
448 M. N., Wang, H., White, T., Wilby, P. R., Woltz, C. R., Wood, R. A., Xiang, L., Yurchenko, I. A.,
449 Zhang, T., Planavsky, N. J., Lau, K. V., Johnston, D. T., and Sperling, E. A.: The Sedimentary
450 Geochemistry and Paleoenvironments Project, *Geobiology*, 19, 545-556,
451 <https://doi.org/10.1111/gbi.12462>, 2021.

452 Gradstein, F. M., Ogg, J. G., Schmitz, M. D., and Ogg, G. M.: *Geologic time scale 2020*, Elsevier, 2020.

453 Granitto, M., Giles, S. A., and Kelley, K. D.: *Global Geochemical Database for Critical Metals in Black*
454 *Shales*, U.S. Geological Survey data release [data set], <https://doi.org/10.5066/F71G0K7X>, 2017.

455 Grossman, E. L. and Joachimski, M. M.: Oxygen Isotope Stratigraphy, in: *Geologic Time Scale 2020*,
456 279-307, <https://doi.org/10.1016/b978-0-12-824360-2.00010-3>, 2020.

457 Jin, C., Li, C., Algeo, T. J., Wu, S., Cheng, M., Zhang, Z., and Shi, W.: Controls on organic matter
458 accumulation on the early-Cambrian western Yangtze Platform, South China, *Mar. Pet. Geol.*, 111,
459 75-87, <https://doi.org/10.1016/j.marpetgeo.2019.08.005>, 2020.

460 Judd, E. J., Tierney, J. E., Huber, B. T., Wing, S. L., Lunt, D. J., Ford, H. L., Inglis, G. N., McClymont,
461 E. L., O'Brien, C. L., Rattanasriampaipong, R., Si, W., Staitis, M. L., Thirumalai, K., Anagnostou,
462 E., Cramwinckel, M. J., Dawson, R. R., Evans, D., Gray, W. R., Grossman, E. L., Henehan, M. J.,
463 Hupp, B. N., MacLeod, K. G., O'Connor, L. K., Sanchez Montes, M. L., Song, H., and Zhang, Y.
464 G.: The PhanSST global database of Phanerozoic sea surface temperature proxy data, *Sci. Data*, 9,
465 753, <https://doi.org/10.1038/s41597-022-01826-0>, 2022.

466 Lai, J., Song, H., Chu, D., Dal Corso, J., Sperling, E. A., Wu, Y., Liu, X., Wei, L., Li, M., Song, H., Du,
467 Y., Jia, E., Feng, Y., Song, H., Yu, W., Liang, Q., Li, X., and Yao, H.: Deep-Time Marine
468 Sedimentary Element Database [data set], Zenodo.
469 <https://doi.org/10.5281/zenodo.13898366><https://doi.org/10.5281/zenodo.14771859>, 2024⁵.

470 Large, R. R., Halpin, J. A., Lounejeva, E., Danyushevsky, L. V., Maslennikov, V. V., Gregory, D., Sack,
471 P. J., Haines, P. W., Long, J. A., Makoundi, C., and Stepanov, A. S.: Cycles of nutrient trace
472 elements in the Phanerozoic ocean, *Gondwana Res.*, 28, 1282-1293,
473 <https://doi.org/10.1016/j.gr.2015.06.004>, 2015.

474 Li, Z., Zhang, Y. G., Torres, M., and Mills, B. J. W.: Neogene burial of organic carbon in the global
475 ocean, *Nature*, 613, 90-95, <https://doi.org/10.1038/s41586-022-05413-6>, 2023.

476 Mackenzie, F. T. and Pigott, J. D.: Tectonic controls of Phanerozoic sedimentary rock cycling, *J. Geol.*
477 *Soc.*, 138, 183-196, <https://doi.org/10.1144/gsjgs.138.2.0183>, 1981.

478 Planavsky, N. J., Asael, D., Rooney, A. D., Robbins, L. J., Gill, B. C., Dehler, C. M., Cole, D. B., Porter,
479 S. M., Love, G. D., Konhauser, K. O., and Reinhard, C. T.: A sedimentary record of the evolution
480 of the global marine phosphorus cycle, *Geobiology*, 21, 168-174, <https://doi.org/10.1111/gbi.12536>,
481 2023.

482 Reinhard, C. T., Planavsky, N. J., Gill, B. C., Ozaki, K., Robbins, L. J., Lyons, T. W., Fischer, W. W.,
483 Wang, C., Cole, D. B., and Konhauser, K. O.: Evolution of the global phosphorus cycle, *Nature*,
484 541, 386-389, <https://doi.org/10.1038/nature20772>, 2017.

485 Schobben, M., Foster, W. J., Sleveland, A. R. N., Zuchuat, V., Svensen, H. H., Planke, S., Bond, D. P.
486 G., Marcelis, F., Newton, R. J., Wignall, P. B., and Poulton, S. W.: A nutrient control on marine

487 anoxia during the end-Permian mass extinction, *Nat. Geosci.*, 13, 640-646,
488 <https://doi.org/10.1038/s41561-020-0622-1>, 2020.

489 Schoepfer, S. D., Algeo, T. J., Ward, P. D., Williford, K. H., and Haggart, J. W.: Testing the limits in a
490 greenhouse ocean: Did low nitrogen availability limit marine productivity during the end-Triassic
491 mass extinction?, *Earth Planet. Sci. Lett.*, 451, 138-148, <https://doi.org/10.1016/j.epsl.2016.06.050>,
492 2016.

493 Schoepfer, S. D., Shen, J., Wei, H., Tyson, R. V., Ingall, E., and Algeo, T. J.: Total organic carbon,
494 organic phosphorus, and biogenic barium fluxes as proxies for paleomarine productivity, *Earth Sci.*
495 *Rev.*, 149, 23-52, <https://doi.org/10.1016/j.earscirev.2014.08.017>, 2015.

496 Scotese, C.: The PALEOMAP Project PaleoAtlas for ArcGIS, version 1, 2, 16-31, 2008.

497 Scotese, C. R., Song, H., Mills, B. J. W., and van der Meer, D. G.: Phanerozoic paleotemperatures: The
498 earth's changing climate during the last 540 million years, *Earth Sci. Rev.*, 215, 103503,
499 <https://doi.org/10.1016/j.earscirev.2021.103503>, 2021.

500 Scotese, C. R. and Wright, N.: PALEOMAP Paleodigital Elevation Models (PaleoDEMS) for the
501 Phanerozoic PALEOMAP Project, Paleomap Proj, [https://www.earthbyte.org/paleodem-](https://www.earthbyte.org/paleodem-resourcescotese-and-wright-2018/)
502 [resourcescotese-and-wright-2018/](https://www.earthbyte.org/paleodem-resourcescotese-and-wright-2018/), 2018.

503 Scott, C., Planavsky, N. J., Dupont, C. L., Kendall, B., Gill, B. C., Robbins, L. J., Husband, K. F., Arnold,
504 G. L., Wing, B. A., Poulton, S. W., Bekker, A., Anbar, A. D., Konhauser, K. O., and Lyons, T. W.:
505 Bioavailability of zinc in marine systems through time, *Nat. Geosci.*, 6, 125-128,
506 <https://doi.org/10.1038/ngeo1679>, 2012.

507 Shen, J., Schoepfer, S. D., Feng, Q., Zhou, L., Yu, J., Song, H., Wei, H., and Algeo, T. J.: Marine
508 productivity changes during the end-Permian crisis and Early Triassic recovery, *Earth Sci. Rev.*,
509 149, 136-162, <https://doi.org/10.1016/j.earscirev.2014.11.002>, 2015.

510 Song, H., Wignall, P. B., Song, H., Dai, X., and Chu, D.: Seawater Temperature and Dissolved Oxygen
511 over the Past 500 Million Years, *J. Earth Sci.*, 30, 236-243, [https://doi.org/10.1007/s12583-018-](https://doi.org/10.1007/s12583-018-1002-2)
512 [1002-2](https://doi.org/10.1007/s12583-018-1002-2), 2019.

513 Stockey, R. G., Cole, D. B., Farrell, U. C., Agic, H., Boag, T. H., Brocks, J. J., Canfield, D. E., Cheng,
514 M., Crockford, P. W., Cui, H., Dahl, T. W., Del Mouro, L., Dewing, K., Dornbos, S. Q., Emmings,
515 J. F., Gaines, R. R., Gibson, T. M., Gill, B. C., Gilleaudeau, G. J., Goldberg, K., Guilbaud, R.,
516 Halverson, G., Hammarlund, E. U., Hantsoo, K., Henderson, M. A., Henderson, C. M., Hodgskiss,

517 M. S. W., Jarrett, A. J. M., Johnston, D. T., Kabanov, P., Kimmig, J., Knoll, A. H., Kunzmann, M.,
518 LeRoy, M. A., Li, C., Loydell, D. K., Macdonald, F. A., Magnall, J. M., Mills, N. T., Och, L. M.,
519 O'Connell, B., Pagès, A., Peters, S. E., Porter, S. M., Poulton, S. W., Ritzer, S. R., Rooney, A. D.,
520 Schoepfer, S., Smith, E. F., Strauss, J. V., Uhlein, G. J., White, T., Wood, R. A., Woltz, C. R.,
521 Yurchenko, I., Planavsky, N. J., and Sperling, E. A.: Sustained increases in atmospheric oxygen
522 and marine productivity in the Neoproterozoic and Palaeozoic eras, *Nat. Geosci.*, 17, 667-674,
523 <https://doi.org/10.1038/s41561-024-01479-1>, 2024.

524 Sweere, T. C., Dickson, A. J., and Vance, D.: Nickel and zinc micronutrient availability in Phanerozoic
525 oceans, *Geobiology*, 21, 310-322, <https://doi.org/10.1111/gbi.12541>, 2023.

526 Tribovillard, N.: Re-assessing copper and nickel enrichments as paleo-productivity proxies, *BSGF -*
527 *Earth Sciences Bulletin*, 192, 54, <https://doi.org/10.1051/bsgf/2021047>, 2021.

528 Veizer, J. and Prokoph, A.: Temperatures and oxygen isotopic composition of Phanerozoic oceans, *Earth*
529 *Sci. Rev.*, 146, 92-104, <https://doi.org/10.1016/j.earscirev.2015.03.008>, 2015.

530 Walker, L. J., Wilkinson, B. H., and Ivany, L. C.: Continental drift and Phanerozoic carbonate
531 accumulation in shallow-shelf and deep-marine settings, *J. Geol.*, 110, 75-87,
532 <https://doi.org/10.1086/324318>, 2002.

533 Wang, D., Liu, Y., Zhang, J., Lang, Y., Li, Z., Tong, Z., Xu, L., Su, Z., and Niu, J.: Controls on marine
534 primary productivity variation and organic matter accumulation during the Late Ordovician – Early
535 Silurian transition, *Mar. Pet. Geol.*, 142, 105742, <https://doi.org/10.1016/j.marpetgeo.2022.105742>,
536 2022.

537 Wilkinson, M. D., Dumontier, M., Aalbersberg, I. J., Appleton, G., Axton, M., Baak, A., Blomberg, N.,
538 Boiten, J. W., da Silva Santos, L. B., Bourne, P. E., Bouwman, J., Brookes, A. J., Clark, T., Crosas,
539 M., Dillo, I., Dumon, O., Edmunds, S., Evelo, C. T., Finkers, R., Gonzalez-Beltran, A., Gray, A. J.,
540 Groth, P., Goble, C., Grethe, J. S., Heringa, J., t Hoen, P. A., Hooft, R., Kuhn, T., Kok, R., Kok, J.,
541 Lusher, S. J., Martone, M. E., Mons, A., Packer, A. L., Persson, B., Rocca-Serra, P., Roos, M., van
542 Schaik, R., Sansone, S. A., Schultes, E., Sengstag, T., Slater, T., Strawn, G., Swertz, M. A.,
543 Thompson, M., van der Lei, J., van Mulligen, E., Velterop, J., Waagmeester, A., Wittenburg, P.,
544 Wolstencroft, K., Zhao, J., and Mons, B.: The FAIR Guiding Principles for scientific data
545 management and stewardship, *Sci. Data*, 3, 160018, <https://doi.org/10.1038/sdata.2016.18>, 2016.

546 Xiang, L., Schoepfer, S. D., Zhang, H., Cao, C., and Shen, S.: Evolution of primary producers and

547 productivity across the Ediacaran-Cambrian transition, *Precambrian Res.*, 313, 68-77,
548 <https://doi.org/10.1016/j.precamres.2018.05.023>, 2018.

549 Zhang, Q., Bendif, E. M., Zhou, Y., Nevado, B., Shafiee, R., and Rickaby, R. E. M.: Declining metal
550 availability in the Mesozoic seawater reflected in phytoplankton succession, *Nat. Geosci.*, 15, 932-
551 941, <https://doi.org/10.1038/s41561-022-01053-7>, 2022.

552 Zhao, K., Zhu, G., Li, T., Chen, Z., and Li, S.: Fluctuations of continental chemical weathering control
553 primary productivity and redox conditions during the Earliest Cambrian, *Geol. J.*, 58, 3659-3672,
554 <https://doi.org/3659-3672>, [10.1002/gj.4778](https://doi.org/10.1002/gj.4778), 2023.